INTERNATIONAL JOURNAL FOR NUMERICAL METHODS IN ENGINEERING
Int. J. Numer. Meth. Engng 2003; **58**:2103–2130 (DOI: 10.1002/nme.847)

Hierarchic finite element bases on unstructured tetrahedral meshes

Mark Ainsworth*,† and Joe Coyle

Mathematics Department, Strathclyde University, 26 Richmond Street, Glasgow G1 1XH, U.K.

SUMMARY

The problem of constructing hierarchic bases for finite element discretization of the spaces H^1, $\mathbf{H}(\mathbf{curl})$, $\mathbf{H}(\mathbf{div})$ and L_2 on tetrahedral elements is addressed. A simple and efficient approach to ensuring conformity of the approximations across element interfaces is described. Hierarchic bases of arbitrary polynomial order are presented. It is shown how these may be used to construct finite element approximations of arbitrary, non-uniform, local order approximation on unstructured meshes of curvilinear tetrahedral elements. Copyright © 2003 John Wiley & Sons, Ltd.

KEY WORDS: hierarchic finite element bases; conforming finite element spaces

1. INTRODUCTION

The variational formulation of partial differential equations arising in science and engineering generally involves one or more of the function spaces $H^1(\Omega)$, $\mathbf{H}(\mathbf{curl};\Omega)$, $\mathbf{H}(\mathbf{div};\Omega)$ and $L_2(\Omega)$. The spaces differ in the smoothness properties required of their members. The space $L_2(\Omega)$ involves the comparatively modest requirement that its members should be square integrable, while the space $H^1(\Omega)$ in addition requires all components of the gradients to be square integrable. The spaces $\mathbf{H}(\mathbf{curl};\Omega)$ and $\mathbf{H}(\mathbf{div};\Omega)$ consist of vector-valued functions and fall in between L_2 and H^1 in the smoothness requirements by asking that certain combinations of first derivatives are square integrable:

$$\mathbf{H}(\mathbf{curl};\Omega)=\{\mathbf{v}\in\mathbf{L}_2(\Omega):\mathbf{curl}\,\mathbf{v}\in\mathbf{L}_2(\Omega)\}$$

and

$$\mathbf{H}(\mathbf{div};\Omega)=\{\mathbf{v}\in\mathbf{L}_2(\Omega):\mathbf{div}\,\mathbf{v}\in L_2(\Omega)\}$$

*Correspondence to: M. Ainsworth, Mathematics Department, Strathclyde University, 26 Richmond Street, Glasgow G1 1XH, U.K.
†E-mail: m.ainsworth@strath.ac.uk

Contract/grant sponsor: Engineering and Physical Sciences Research Council of Great Britain; contract/grant number: GR/M59426

Received 15 May 2002
Revised 17 January 2003
Accepted 24 March 2003

The finite element method is frequently used to approximate the solutions of boundary value problems. A family of finite element subspaces should respect the smoothness requirements of the underlying function space associated with the problem to be approximated. The most commonly occurring case involves the space $H^1(\Omega)$ where the smoothness requirements translate into the fact that a finite element subspace must consist of functions that are continuous across inter-element boundaries. At the opposite extreme the space $L_2(\Omega)$, which frequently occurs in the setting of mixed finite element schemes, imposes no inter-element continuity requirements on the finite element subspace.

The spaces $\mathbf{H}(\mathbf{curl};\Omega)$ and $\mathbf{H}(\mathbf{div};\Omega)$, although less common, are nevertheless of considerable importance in application areas such as electromagnetism, elasticity and fluid mechanics. The inter-element continuity requirements or *conformity* conditions are more complicated for these spaces. The space $\mathbf{H}(\mathbf{div};\Omega)$ requires the normal component of the finite element function to be continuous across an interface, while the space $\mathbf{H}(\mathbf{curl};\Omega)$ requires that certain tangential components of the finite element approximation should be continuous. These conditions are weaker than those associated with the space $H^1(\Omega)$, but their realisation can prove problematic nevertheless. One possible alternative consists of using the more familiar vector-valued $\mathbf{H}^1(\Omega)$-conforming finite element space in place of an $\mathbf{H}(\mathbf{div};\Omega)$ or $\mathbf{H}(\mathbf{curl};\Omega)$-conforming approximation. Unfortunately, this means that the approximation is overly constrained and opens up the possibility that the finite element scheme may not actually converge to the solution of the problem in hand.

The construction of low order $\mathbf{H}(\mathbf{div})$ and $\mathbf{H}(\mathbf{curl})$ conforming approximation may be found in textbooks [1–4]. However, interest in the use of higher order finite element schemes, such as p, hp or spectral element methods, has become increasingly widespread. These methods typically involve the use of elements of variable, non-uniform order approximation on unstructured meshes [5, 6]. The use of a higher order space can lead to complications with enforcing appropriate conformity properties of globally defined basis functions across element interfaces, particularly if elements of non-uniform local order are employed.

The treatment of the L_2 and H^1-conforming finite element spaces is well documented in the literature. For example, sets of hierarchic basis functions of arbitrary order on tetrahedral elements may be found in the books of Szabo and Babuska [6], and Karniadakis and Sherwin [7]. These spaces are also discussed in the present work, partly in the interests of completeness and partly in order to set the work in context. However, our main reason for revisiting these simpler spaces is to highlight in a familiar setting some of the difficulties which, though not always apparent, are the crux of the problem of constructing conforming spaces on unstructured meshes.

A survey of (low order) finite element schemes geared towards h-version discretization of $\mathbf{H}(\mathbf{div})$, and to a lesser extent $\mathbf{H}(\mathbf{curl})$, may be found in the book of Brezzi and Fortin [2]. The basic framework for finite element spaces of arbitrary order on tetrahedral elements was described by Nédélec [8, 9]. The work of Hiptmair [10] is remarkable in that it encompasses a unified treatment of finite element discretization of both spaces $\mathbf{H}(\mathbf{curl})$ and $\mathbf{H}(\mathbf{div})$ within the framework of differential forms.

The lowest order finite element schemes for the discretization of $\mathbf{H}(\mathbf{curl})$ are often referred to as *edge elements* [11–13] or *Whitney forms* [14]. The search for a convenient set of basis functions for higher order approximation has attracted a great deal of attention. Several variants of second order basis functions have been described in References [15–18], while third order elements have been considered in References [19–22]. A hierarchic set of basis

functions up to third order has been presented by Webb and Forghani [23] while Anderson and Volakis [24] target efforts on the construction of higher order functions based on the Whitney forms. The construction of elements of higher than third order is considered by Graglia *et al.* [25] where a nodal basis is described, and Webb [26] where basis functions of arbitrary order are presented based on the degrees of freedom outlined in Reference [9]. Demkowicz and Vardapetyan [27] derived families of non-uniform arbitrary order spaces for $\mathbf{H}(\mathbf{curl})$ and $\mathbf{H}(\mathbf{div})$ and showed [27] that the vital commuting diagram property [2] is preserved.

Despite the intensive search for hierarchic bases for arbitrary order finite element discretization of the spaces $\mathbf{H}(\mathbf{curl})$ and $\mathbf{H}(\mathbf{div})$, a number of problems remain with the realisation. Most, if not all, of the existing works are limited to low order elements of uniform degree and focus on describing the basis functions on a reference tetrahedron devoting little attention to the problem of ensuring that the associated global basis functions satisfy the global conformity conditions. However, the work of Demkowicz *et al.* [27, 28], deals with approximation of arbitrary order. The problem of deriving bases for non-uniform order approximation of $\mathbf{H}(\mathbf{curl})$ and $\mathbf{H}(\mathbf{div})$ in two dimensions on hybrid meshes of triangular and quadrilateral elements was studied in Reference [29].

The purpose of the current work is to obtain families of hierarchic basis functions of arbitrary polynomial order and to describe the process whereby these functions may be used to construct arbitrary, non-uniform local polynomial order finite element subspaces for $H^1(\Omega)$, $\mathbf{H}(\mathbf{curl};\Omega)$, $\mathbf{H}(\mathbf{div};\Omega)$ and $L_2(\Omega)$ on general unstructured meshes of possibly curvilinear tetrahedra. Thus, the current work presents a reasonably complete solution to the problem of developing bases on tetrahedral meshes, although some important issues such as conditioning of the matrices are not addressed.

The remainder of the manuscript is organized as follows. Firstly, the problem of enforcing continuity across element boundaries on an unstructured mesh of tetrahedral elements is discussed. Fully hierarchic bases of arbitrary uniform polynomial order are then exhibited for the four spaces of interest. Finally, the generalization to non-uniform local order of approximation is discussed along with the details of the implementation.

2. THE PROBLEM OF ENFORCING CONFORMITY

Traditionally, finite elements as described, for example by Ciarlet [30], are constructed with degrees of freedom identified with the values of a function, or appropriate derivatives, at nodes located on the element. However, when higher or non-uniform local orders are required, as is the case for the *hp*-version finite element method, it is advantageous to use degrees of freedom corresponding to hierarchic basis functions [6, 31]. Unfortunately, hierarchic bases create problems with enforcing conformity of the approximation across element interfaces that do not arise with the traditional nodal bases. Here, we illustrate the types of problem that arise in the setting of the scalar $H^1(\Omega)$ space. Similar, but more acute, difficulties are encountered in the finite element discretization of the spaces $\mathbf{H}(\mathbf{curl})$ and $\mathbf{H}(\mathbf{div})$.

2.1. Enforcing $H^1(\Omega)$-conformity in two dimensions

Suppose that the polygonal domain Ω is partitioned into triangles so that the non-empty intersection of distinct elements is a single common edge or vertex of both elements. Consider

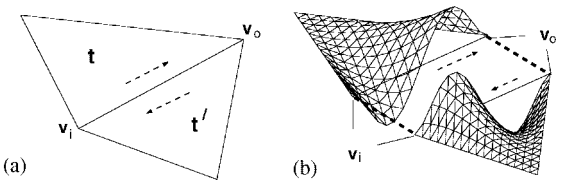

Figure 1. (a) Triangular elements $\mathbf{t}$ and $\mathbf{t}'$ sharing a common edge $\mathbf{e}$ connecting the vertices $\mathbf{v}_o$ and $\mathbf{v}_i$. The local orientation of the edge within each element is indicated by the dashed arrows; and (b) local cubic edge basis functions on each element. The mismatch in the local orientation of the edges means that the values of the local degrees of freedom corresponding to the edge function must be appropriately constrained to ensure conformity.

the situation where the order of approximation is chosen to be cubic, $p=3$, and let u be a function from the finite element space. The restriction of u to an inter-element edge $\mathbf{e}$ shared by elements $\mathbf{t}$ and $\mathbf{t}'$ (see Figure 1) will be a cubic function of the parametrization $\xi \in [-1,1]$ used on the edge.

Traditionally, the function would be described by values at four nodes on the edge and these values would correspond to values of local degrees of freedom on both elements $\mathbf{t}$ and $\mathbf{t}'$. The situation is rather different when a hierarchic basis is employed. For instance, a natural choice of hierarchic basis functions, when restricted to the edge, would give the functions

$$\tfrac{1}{2}(1-\xi); \quad \tfrac{1}{2}(1+\xi); \quad 1-\xi^2; \quad \xi(1-\xi^2) \tag{1}$$

If the local orientation of the edges on the reference element is chosen so that the boundary is traversed in an anti-clockwise sense, then the local orientations of the common edge are mismatched, as shown in Figure 1(a). As a consequence, the local parametrization of the edges in each element, denoted by $\xi_{\mathbf{t}}$ and $\xi_{\mathbf{t}'}$, satisfies $\xi_{\mathbf{t}} = -\xi_{\mathbf{t}'}$. This creates difficulties in enforcing continuity across the edge. For instance, suppose u vanishes at the endpoints of the edge $\mathbf{e}$ so that the first two functions in (1) are redundant. Relative to the basis functions on element $\mathbf{t}$, the restriction of u to the edge is given by

$$u|_{\mathbf{e}} = c_0(1-\xi_{\mathbf{t}}^2) + c_1\xi_{\mathbf{t}}(1-\xi_{\mathbf{t}}^2)$$

while relative to element $\mathbf{t}'$

$$u|_{\mathbf{e}} = c_0'(1-\xi_{\mathbf{t}'}^2) + c_1'\xi_{\mathbf{t}'}(1-\xi_{\mathbf{t}'}^2)$$

In order to obtain a conforming approximation, the values of these different representations must agree on the interface. Inserting $\xi_{\mathbf{e}'} = -\xi_{\mathbf{e}}$ into the latter equation and comparing coefficients leads to the conclusion

$$\begin{aligned} c_0 &= c_0' \\ c_1 &= -c_1' \end{aligned} \tag{2}$$

The reason behind the sign difference is illustrated in Figure 1(b) where the restrictions of the local cubic edge basis function on the edge are shown. It is observed that the cubic modes have differing signs due to the mismatch in the local orientations of the edge.

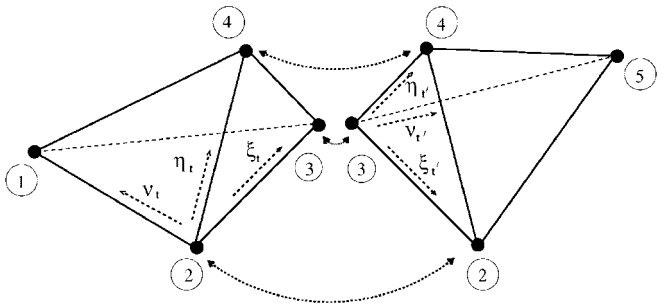

Figure 2. The pair of adjacent tetrahedra, $\mathbf{t} = [2\,3\,1\,4]$ and $\mathbf{t}' = [3\,4\,2\,5]$, sharing a common face $\mathbf{f}$ defined by the vertices with global numbers 2, 3 and 4. The natural coordinates for each element are indicated by the dashed arrows.

The need to resolve such *sign conflicts* [31] is typical when hierarchic basis functions are used, but does not arise for nodal basis functions. While it is a relatively trivial matter to apply these constraints by incorporating a sign change in the local–global (connectivity) mapping for the element [32], the situation in three dimensions is not so simple.

2.2. *Enforcing $H^1(\Omega)$-conformity in three dimensions*

The basic difficulty in enforcing $H^1(\Omega)$-conformity in three dimensions first manifests itself in the simple case where fourth order, $p = 4$, elements are used and the domain Ω consists of only two elements. Such a situation is shown in Figure 2, where the tetrahedra, $\mathbf{t}$ and $\mathbf{t}'$, share a common face $\mathbf{f}$ defined by nodes with global numbers 2, 3 and 4.

If the boundary value problem is subject to homogeneous boundary conditions, then the finite element functions must vanish on the boundary of the domain Ω. Let λ_2, λ_3 and λ_4 denote the usual barycentric, or area, coordinates. A cubic finite element function that vanishes on the boundary of the face $\mathbf{f}$, but is non-zero on the face itself, must be a multiple of the polynomial $\beta_{\mathbf{f}}$ given by $\lambda_2\lambda_3\lambda_4$. Consequently, on the face $\mathbf{f}$, the basis for the third order space must reduce to a multiple of the function $\beta_{\mathbf{f}}$.

If the order of approximation is increased to fourth order, $p = 4$, and a hierarchic basis is required, then the basis functions on the face must, in addition to the function $\beta_{\mathbf{f}}$, include two further functions of the form $\beta_{\mathbf{f}} w$, where w is an affine function. The natural choice for the two additional functions on element $\mathbf{t}$ corresponds to taking w to be $\xi_{\mathbf{t}}$ and $\eta_{\mathbf{t}}$, as shown in Figure 2, giving the following local face basis functions on element $\mathbf{t}$:

$$\beta_{\mathbf{f}}; \quad \beta_{\mathbf{f}}\xi_{\mathbf{t}}; \quad \beta_{\mathbf{f}}\eta_{\mathbf{t}}$$

By the same token, the local face basis functions on $\mathbf{t}'$ are given by

$$\beta_{\mathbf{f}}; \quad \beta_{\mathbf{f}}\xi_{\mathbf{t}'}; \quad \beta_{\mathbf{f}}\eta_{\mathbf{t}'}$$

A quartic finite element function u that is non-zero on the face $\mathbf{f}$, relative to the basis functions for element $\mathbf{t}$, has the form

$$u|_{\mathbf{f}} = \beta_{\mathbf{f}}(c_0 + c_1\xi_{\mathbf{t}} + c_2\eta_{\mathbf{t}}) \tag{3}$$

whilst relative to element $\mathbf{t}'$, the function has the form

$$u|_{\mathbf{f}} = \beta_{\mathbf{f}}(c_0' + c_1'\xi_{\mathbf{t}'} + c_2'\eta_{\mathbf{t}'}) \tag{4}$$

The relationship between the coefficients needed to ensure agreement on the face can be deduced by first observing that

$$\xi_{\mathbf{t}'} = \lambda_2; \quad \eta_{\mathbf{t}'} = \lambda_4$$

or, noting that $\lambda_2 + \lambda_3 + \lambda_4 = 1$ on $\mathbf{f}$,

$$\xi_{\mathbf{t}'} = 1 - \lambda_3 - \lambda_4; \quad \eta_{\mathbf{t}'} = \lambda_4$$

Similarly,

$$\xi_{\mathbf{t}} = \lambda_3; \quad \eta_{\mathbf{t}} = \lambda_4$$

and so, inserting these into Equations (3)–(4) and equating coefficients, we obtain

$$\begin{aligned} c_0 &= c_0' + c_1' \\ c_1 &= -c_1' \\ c_2 &= -c_1' + c_2' \end{aligned} \tag{5}$$

By way of contrast to the two dimensional case, the application of these constraints is no longer simply a matter of resolving sign conflicts. Indeed, the non-local nature of the constraints makes even the task of identifying the global degrees of freedom non-trivial.

The source of the difficulty may be traced to the freedom in the choice of the *two* functions needed to augment the basis function already present in the cubic space, to form a basis for the fourth order space. This leads to a set of face basis functions that do not remain invariant under a cycling of the numbering of the vertices on the face. This, in turn, is responsible for the more complicated, non-local constraints (5). It is not difficult to convince oneself of the impossibility of constructing hierarchic basis while maintaining *rotational invariance*. In contrast, a natural choice of nodal basis is automatically rotationally invariant and non-local constraints do not arise. The subject of rotational invariance is discussed further by Webb [26].

2.3. *Circumventing sign conflicts*

The foregoing discussion shows that a hierarchic, conforming basis in two dimensions can be realized purely by resolving sign conflicts. However, this notion does not generalize to the three dimensional case due to the loss of rotational invariance in the face basis functions. Faced with this impasse, we shall revisit the two dimensional case in search of an alternative concept that is more readily extended to the three dimensional setting.

Akin [31] shows that, in two dimensions, it is possible to avoid sign conflicts altogether by employing a consistent orientation of edges. An edge $\mathbf{e}$ connecting the global vertices $\mathbf{v}_o$ and $\mathbf{v}_i$, is assigned a unique, global orientation by choosing, for instance, the tangent vector in the direction from the vertex $\mathbf{v}_o$ to vertex $\mathbf{v}_i$. The associated parametrization of the edge is given by $\xi_{oi} = \lambda_i - \lambda_o \in [-1, 1]$, as shown in Figure 3(a). The local parametrization of the edge in the reference element is chosen to coincide with the global parametrization of the edge.

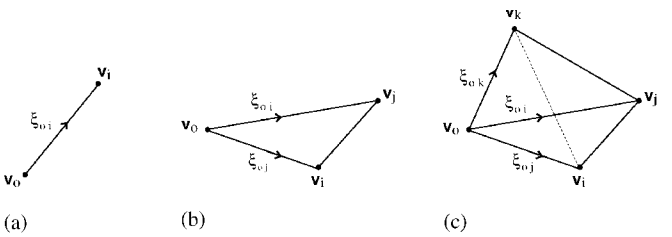

Figure 3. Intrinsic orientations of entities based on the global numbering of the vertices defining the entity. Here, it is assumed that the global numbering satisfies $o<i<j<k$. In each case, the vertex $\mathbf{v}_o$ with the lowest global numbering is singled out as the preferred vertex: (a) edge orientation; (b) face orientation; and (c) tetrahedral orientation.

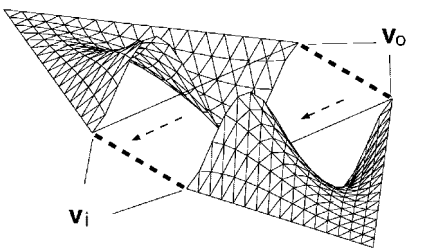

Figure 4. The continuity of the global cubic functions across $\mathbf{e}$ is a consequence of a consistent local parametrization of each edge from the smallest vertex $\mathbf{v}_o$ to the largest vertex $\mathbf{v}_i$ on both elements.

This process circumvents the sign conflict problem. Consider once again the example illustrated in Figure 1. The common edge $\mathbf{e}=[o\ i]$ would be oriented in the same direction on both triangles. The local parametrization ξ_{oi} used to define the local basis functions would then agree on neighbouring elements, and the cubic edge function would automatically be continuous across $\mathbf{e}$, as shown in Figure 4. In particular, the constraints (2) would then take the form

$$c_0 = c_0'$$

$$c_1 = c_1'$$

and the issue of sign conflicts no longer arises.

The same notion may be used in three dimensions to circumvent the problem of rotational invariance in enforcing $H^1(\Omega)$-conformity across faces. A face $\mathbf{f}=[o\ i\ j]$ defined by global vertices $\mathbf{v}_o$, $\mathbf{v}_i$ and $\mathbf{v}_j$ is parameterised by choosing coordinates $\xi_{oi}=\lambda_i-\lambda_o$ and $\xi_{oj}=\lambda_j-\lambda_o$, as shown in Figure 3(b). The local parametrization of the face on the reference element is chosen to agree with the global parametrization.

Consider once again the situation shown in Figure 2. The face basis functions for the fourth order space are chosen to be of the same form on *both* elements:

$$\beta_{\mathbf{f}};\quad \beta_{\mathbf{f}}\xi_{23}=\beta_{\mathbf{f}}(\lambda_3-\lambda_2);\quad \beta_{\mathbf{f}}\xi_{24}=\beta_{\mathbf{f}}(\lambda_4-\lambda_2)$$

With this choice of basis, the arguments leading to conditions (5) would yield the trivial set of constraints

$$c_0 = c_0'; \quad c_1 = c_1'; \quad c_2 = c_2'$$

and conformity is obtained automatically. In short, once a unique global preferred parametrization of the faces has been defined, the same parametrization may be adopted locally on each element and issues of rotational invariance become irrelevant.

2.4. Intrinsic orientation of edges and faces

The foregoing examples illustrate that the orientation of the element faces and edges is the key to enforcing appropriate continuity properties of the discrete spaces. It is important that the method chosen to orient faces and edges can be applied locally on each element in isolation, without the need to refer to exterior entities such as the elements containing them.

Denote the set of vertices, edges and faces of a single element $\mathbf{t}$ by $\mathscr{V}(\mathbf{t})$, $\mathscr{E}(\mathbf{t})$ and $\mathscr{F}(\mathbf{t})$, respectively, and the corresponding global sets by $\mathscr{V}$, $\mathscr{E}$ and $\mathscr{F}$.

Each edge $\mathbf{e} \in \mathscr{E}$ is described by a pair $[o\ i]$ of numbers for the global vertices located at the endpoints of the edge. The ordering of the numbers is determined by requiring $o < i$. The edge may then be assigned a unique parametrization given by

$$\xi_{\mathbf{e}} : \mathbb{R}^3 \to \mathbb{R}: \quad \xi_{\mathbf{e}} = \xi_{oi} = \lambda_i - \lambda_o \tag{6}$$

The parametrization is intrinsic to the edge, depending solely on the global numbering of the endpoints of the edge.

Likewise, a face $\mathbf{f} \in \mathscr{F}$ is described by a triple $[o\ i\ j]$ formed from the global numbering of the vertices of the face. By applying a rotation of the local numbering of the vertices, it is possible to ensure that the vertex $\mathbf{v}_o$ with the smallest global numbering, has local number 1 without affecting the properties of the face itself. The ordering of the remaining vertices, $\mathbf{v}_i$ and $\mathbf{v}_j$, is then automatically determined so that the cyclic ordering of the vertices is preserved. This process results in a well-defined ordering of the vertices. The face is then assigned a unique parametrization given by ξ_{oi} and ξ_{oj}. Once again, the parametrization is intrinsic to the face and is determined entirely in terms of the global numbering of the vertices of the face. Equally well, a tetrahedron $\mathbf{t} = [o\ i\ j\ k] \in \mathscr{T}$ is parametrized by ξ_{oi}, ξ_{oj} and ξ_{ok}, as shown in Figure 3. The ordering of the vertices in the tetrahedron is discussed in detail in the next section.

A unique directed tangent on an edge $\mathbf{e} = [o\ i]$ is given by

$$\boldsymbol{\tau}^{\mathbf{e}} = \boldsymbol{\tau}^{[oi]} = \mathbf{v}_i - \mathbf{v}_o \tag{7}$$

while a unique pair of tangent vectors to face $\mathbf{f} = [o\ i\ j]$ is defined by

$$\boldsymbol{\tau}_1^{\mathbf{f}} = \boldsymbol{\tau}^{[oi]} \quad \text{and} \quad \boldsymbol{\tau}_2^{\mathbf{f}} = \boldsymbol{\tau}^{[oj]} \tag{8}$$

For future reference, we introduce *bubble* functions on each edge $\mathbf{e}$, face $\mathbf{f}$ and tetrahedron $\mathbf{t}$ by

$$\beta_{\mathbf{e}} = \beta_{oi} = \lambda_o \lambda_i; \quad \beta_{\mathbf{f}} = \beta_{oij} = \lambda_o \lambda_i \lambda_j \quad \text{and} \quad \beta_{\mathbf{t}} = \beta_{oijk} = \lambda_o \lambda_i \lambda_j \lambda_k \tag{9}$$

Note that these functions vanish on the boundary of the entity with which they are associated and are therefore continuous functions.

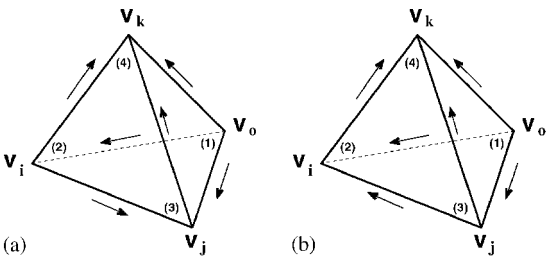

Figure 5. The two possible reference tetrahedra. The arrows indicate the global orientation of the edges. The tetrahedra differ only in the orientation of the edge connecting vertices $\mathbf{v}_i$ and $\mathbf{v}_j$, which depends on the ordering of the global numbers i and j. If $i<j$, then the tetrahedron is of Type I, and of Type II otherwise: (a) type I: $i<j$; and (b) type II: $i>j$.

2.5. *Intrinsic orientation of elements*

The intrinsic orientation of the edges and faces described above depends on the global numbering of the vertices. This means that the construction of the basis functions on the reference element also depends on the numbering of the global vertices defining the element. At first sight, this fact appears to carry undesirable consequences. Fortunately, this proves not to be the case thanks to the following key observation: *An appropriate reordering of the local numbering of the vertices allows any global tetrahedron to be reduced to one of two possible reference tetrahedra.* This process will be illustrated below. The significance of the observation is that the standard finite element technology, whereby computations are performed on a corresponding reference element, is not sacrificed provided *two* reference tetrahedra are utilized.

The reduction to one of two reference tetrahedra is achieved by the following procedure:

1. Local vertex 1 is aligned with the smallest global vertex $\mathbf{v}_o$ by rotating the local numbering on either of the two faces containing global vertex $\mathbf{v}_o$ and local vertex 1. (Of course, if the two are already aligned, then no action is needed.)
2. Local vertex 4 is aligned with the largest global vertex $\mathbf{v}_k$ by rotating the local numbering on the face opposite local vertex 1.
3. The tetrahedron is then classified as Type I or II, according to the relative ordering of the global numbering of the remaining vertices $\mathbf{v}_i$ and $\mathbf{v}_j$. If $i<j$, then the tetrahedron is of Type I, and otherwise of Type II (see Figure 5).

As a simple example, consider a tetrahedron with global numbering [15 96 8 24] as shown in Figure 6(a). The general procedure applied to this particular tetrahedron gives:

1. The triple [15 96 8] representing a face containing the smallest global and local vertices, is cyclically permuted until the smallest global vertex has local number 1. This yields [8 15 96] and is equivalent to the rotation of a local face to align the smallest global and local vertices as shown in Figure 6(b). This gives the new local to global numbering [8 15 96 24] for the tetrahedron.
2. The triple [15 96 24] representing the face opposite the smallest local vertex, is cyclically permuted to align global vertex 96 with local vertex 4. This is equivalent to rotating the

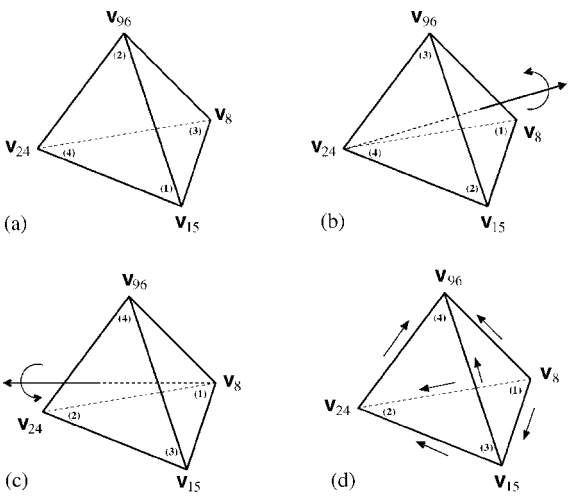

Figure 6. Reduction of tetrahedron with original numbering [15 96 8 24] to Type II reference tetrahedron. The local numbers are shown in parentheses: (a) original numbering of physical tetrahedron [15 96 8 24]; (b) align vertices with smallest local and global numbers by rotating a face containing both vertices, giving the new numbering [8 15 96 24]; (c) align vertices with greatest local and global numbers by rotating the face containing both vertices giving the new numbering [8 24 15 96]; and (d) final alignment of tetrahedron and orientation of edges. The relative ordering of the global numbers for local nodes 2 and 3 corresponds to a Type II element.

local face opposite the smallest local vertex as shown in Figure 6(c). This results in a new local to global mapping [8 24 15 96].

3. This tetrahedron is then classified as a Type II reference element as shown in Figure 5 (because $24 > 15$).

If the original numbering of the tetrahedron is given by [24 96 8 15], then the procedure would result in a numbering given by [8 15 24 96] corresponding to a Type I reference element.

In practice, the reduction to a Type I or II reference configuration is performed as a pre-processing step at a negligible cost. The fact that every element may be reduced to a Type I or II reference element is of vital significance: *Every edge and every face of the appropriate reference configuration is identical with the intrinsic orientations of the edges and faces viewed in isolation.* This means that the parametrization on the reference element will automatically be compatible with the global parametrization of the edges and faces induced by the intrinsic orientation. Consequently, once the tetrahedra have been classified as Type I or II, there is no need to check orientations during the finite element analysis.

3. HIERARCHIC BASES

Hierarchic basis functions are essential for the efficient, practical implementation of higher order finite element methods, such as p and hp-version procedures, where increased accuracy

relies on increasing the order of the polynomial space. Here, we derive hierarchic bases for arbitrary, non-uniform order discretization of the spaces H^1, $\mathbf{H}(\mathbf{curl})$, $\mathbf{H}(\mathbf{div})$ and L_2 on an unstructured partitioning $\mathscr{T}$ of the domain into tetrahedral elements. It is assumed throughout that the partitioning is regular in the sense that the non-empty intersection of distinct elements is either a single common vertex, edge or face of both elements. Non-degenerate curvilinear elements are permitted. In particular, each element $\mathbf{t} \in \mathscr{T}$ is assumed to be the image of a reference tetrahedron $\hat{\mathbf{t}}$ under a smooth bijective mapping $\mathbf{F}_\mathbf{t}$, with the Jacobian of the mapping denoted by $\mathbf{J}_\mathbf{t}$.

A set $\{\psi_\ell : \ell = 0, 1, \ldots\}$ constitutes a hierarchic basis on a reference interval $I = [-1, 1]$ if, for each $\ell = 0, 1, \ldots$, the function ψ_ℓ is a polynomial of degree ℓ. This set will be used to construct general bases on tetrahedra and is referred to as the *primary basis*. One obvious choice for ψ_ℓ would be the monomial of degree ℓ. However, in practice, ψ_ℓ is often taken to be the Legendre polynomial L_ℓ of degree ℓ, defined inductively by the relation

$$\begin{aligned} &L_0(s) = 1; \quad L_1(s) = s \\ &L_{\ell+1}(s) = \frac{2\ell+1}{\ell+1} sL_\ell(s) - \frac{\ell}{\ell+1} L_{l-1}(s), \quad \ell = 1, 2, \ldots \end{aligned} \tag{10}$$

As a matter of fact, any family of polynomials could be chosen, such as the Gegenbauer polynomials [33, Section 8.93] defined, for fixed α, by

$$\begin{aligned} &\psi_0(s) = 1; \quad \psi_1(s) = 2\alpha s \\ &\psi_{\ell+1}(s) = \frac{2(\alpha+\ell)}{\ell+1} s\psi_\ell(s) - \frac{2\alpha+\ell-1}{\ell+1} \psi_{\ell-1}(s), \quad \ell = 1, 2, \ldots \end{aligned} \tag{11}$$

The choice $\alpha = \frac{1}{2}$ gives the Legendre polynomials.

The primary basis for an interval I may be used to construct polynomial bases on edges, faces and interiors by taking the arguments of the primary basis functions to be of the form

$$\xi_{oi} = \lambda_i - \lambda_o \in [-1, 1]$$

as follows:

Lemma 1
Let $\{\psi_\ell : \ell = 0, 1, \ldots\}$ be a hierarchic basis on a reference interval I. Then, bases for the spaces $\mathbb{P}_p$ of polynomials of total degree at most $p \in \mathbb{N}$ on edges, faces and interiors are given by

1. for $\mathbf{e} = [o\ i] \in \mathscr{E}$,

$$\mathbb{P}_p(\mathbf{e}) = \text{span}\{\psi_\ell(\xi_{oi}) : 0 \leqslant \ell \leqslant p\}$$

2. for $\mathbf{f} = [o\ i\ j] \in \mathscr{F}$,

$$\mathbb{P}_p(\mathbf{f}) = \text{span}\{\psi_\ell(\xi_{oi})\psi_m(\xi_{oj}) : 0 \leqslant \ell, m, \ell + m \leqslant p\}$$

Table I. Hierarchic basis functions for L_2-conforming finite element space of order p.

Space: $\mathbb{P}_p(\hat{\mathbf{t}})$, $p \in \mathbb{N}$
Interior functions: $\hat{\mathbf{t}} = [o\ \ i\ \ j\ \ k]$
$\hat{\varphi}^{\hat{\mathbf{t}}}_{\ell mn} = \psi_\ell(\hat{\xi}_{oi})\psi_m(\hat{\xi}_{oj})\psi_n(\hat{\xi}_{ok}), \quad 0 \leqslant \ell, m, n, \ell + m + n \leqslant p$

3. for $\mathbf{t} = [o\ \ i\ \ j\ \ k] \in \mathscr{T}$,

$$\mathbb{P}_p(\mathbf{t}) = \operatorname{span}\{\psi_\ell(\xi_{oi})\psi_m(\xi_{oj})\psi_n(\xi_{ok}) : 0 \leqslant \ell, m, n, \ell + m + n \leqslant p\}$$

The proof of this result is left as an elementary exercise. For future reference it is worth noting that the functions in each of these sets are linearly independent.

3.1. L_2 and H^1-conforming basis functions

A conforming discretization of the space $H^1(\Omega)$ is characterized by continuity (of traces) across element interfaces. By way of contrast, the space L_2 imposes no such continuity requirements on interfaces which simplifies the construction of conforming finite element spaces dramatically.

3.1.1. Reference element basis functions. The polynomial spaces of order p on the reference element $\hat{\mathbf{t}}$ for both the H^1 and L_2 spaces is given by

$$\hat{X}_p^{H^1} = \hat{X}_p^{L_2} = \mathbb{P}_p(\hat{\mathbf{t}})$$

However, the differing continuity requirements on the interfaces mean that different bases are used to realize these spaces. For instance, the set of hierarchic basis functions for $\hat{X}_p^{L_2}$ given in Table I consists entirely of *interior* functions. The term *interior* reflects the nature of the degrees of freedom associated with the functions. The absence of conformity conditions for the space L_2 means that the coefficients of all basis functions can be chosen completely independently on all elements. In this sense, the degrees of freedom are *internal* to the element.

Conversely, the set of hierarchic basis functions for $\hat{X}_p^{H^1}$ based on the primary basis $\{\psi_\ell : \ell \in \mathbb{N}\}$ given in Table II is split into sets of functions identified with element vertices, edges, faces and interiors. This reflects the differing conformity conditions for the space H^1. The requirement for continuity between elements means that the basis functions must match at vertices, on edges and on faces. *Vertex functions* are the only non-zero functions at element vertices and therefore must have the same coefficient on all elements containing the vertex. Similarly, *edge functions* are (apart from the vertex functions) the only non-zero functions on element edges and must have identical coefficients on all elements containing the edge. Equally well, the coefficients of the *face functions* need only match on the pair of elements sharing the common face. Finally, *interior functions* vanish on all shared boundaries and their coefficients may be chosen independently on each element.

It will be observed that the nature of a function depends on the particular space under consideration. The same function could be an interior function for the L_2 case but need not

Table II. Hierarchic basis functions for H^1-conforming finite element space of order p.

Space: $\mathbb{P}_p(\hat{\mathbf{t}}),\ p \in \mathbb{N}$
Vertex functions: $\mathbf{v} \in \mathscr{V}(\hat{\mathbf{t}})$
$\hat{\varphi}^{\mathbf{v}} = \hat{\lambda}_{\mathbf{v}}$
Edge functions: $\mathbf{e} = [o\ \ i] \in \mathscr{E}(\hat{\mathbf{t}})$
$\hat{\varphi}^{\mathbf{e}}_{\ell} = \beta_{oi}\psi_{\ell}(\hat{\xi}_{oi}), \quad 0 \leqslant \ell \leqslant p-2$
Face functions: $\mathbf{f} = [o\ \ i\ \ j] \in \mathscr{F}(\hat{\mathbf{t}})$
$\hat{\varphi}^{\mathbf{f}}_{\ell m} = \beta_{oij}\psi_{\ell}(\hat{\xi}_{oi})\psi_m(\hat{\xi}_{oj}), \quad 0 \leqslant \ell, m,\ \ell + m \leqslant p-3$
Interior functions: $\hat{\mathbf{t}} = [o\ \ i\ \ j\ \ k]$
$\hat{\varphi}^{\hat{\mathbf{t}}}_{\ell mn} = \beta_{oijk}\psi_{\ell}(\hat{\xi}_{oi})\psi_m(\hat{\xi}_{oj})\psi_n(\hat{\xi}_{ok}), \qquad 0 \leqslant \ell, m, n, \ell + m + n \leqslant p-4$

necessarily be an interior function for the H^1 space. For instance, an interior function for the space L_2 need not vanish on element boundaries.

Lemma 2
The set of functions defined in Tables I and II forms a hierarchic basis for the spaces $\hat{X}_p^{H^1}$ and $\hat{X}_p^{L_2},\ p \in \mathbb{N}$, respectively.

Proof
Let $p \in \mathbb{N}$. The result in case of the space L_2 is an immediate consequence of Lemma 1. The H^1 case requires some attention. The vertex function $\hat{\varphi}^{\mathbf{v}}$ belongs to $\mathbb{P}_1$ and, *a fortiori*, $\mathbb{P}_p$. Consider an edge function $\hat{\varphi}^{\mathbf{e}}_{\ell}$, $\ell \in \{0, \ldots, p-2\}$. By definition, ψ_{ℓ} is a degree ℓ polynomial, and so, since $\xi_{ij} = \lambda_j - \lambda_i \in \mathbb{P}_1$, it follows that the function $\psi_{\ell}(\xi_{ij})$ belongs to $\mathbb{P}_{\ell}$. Consequently, the edge function $\hat{\varphi}^{\mathbf{e}}_{\ell}$ belongs to $\mathbb{P}_{\ell+2}$ and hence also belongs to $\mathbb{P}_p$ since $\ell \leqslant p-2$. Similar arguments show that the face and interior functions also belong to the space $\mathbb{P}_p$.

The functions are linearly independent. For instance, suppose

$$\sum_{\mathbf{v} \in \mathscr{V}} w_{\mathbf{v}} + \sum_{\mathbf{e} \in \mathscr{E}} w_{\mathbf{e}} + \sum_{\mathbf{f} \in \mathscr{F}} w_{\mathbf{f}} + w_{\mathbf{t}} \equiv 0 \tag{12}$$

where $w_{\mathbf{v}} \in \operatorname{span}\{\hat{\varphi}^{\mathbf{v}}\}$, etc. The presence of the edge, face and interior bubble functions in the definitions means that $\sum_{\mathbf{v} \in \mathscr{V}} w_{\mathbf{v}}$ vanishes at the element vertices. Consequently, since the barycentric coordinate functions are linearly independent, each term $w_{\mathbf{v}}$ vanishes and it follows that the first term in Equation (12) is identically zero. The only remaining term in (12) that is non-zero on the element edge $\mathbf{e}$ is $w_{\mathbf{e}} \in \beta_{\mathbf{e}} \operatorname{span}\{\psi_{\ell}\}$. It follows that $w_{\mathbf{e}}$ must vanish identically since $\{\psi_{\ell}\}$ forms a basis on an interval. Consequently, the second term in (12) vanishes. Similarly, $w_{\mathbf{f}}$ vanishes on the face $\mathbf{f}$, and analogous arguments show $w_{\mathbf{f}}$ must therefore be identically zero. Finally, it follows that $w_{\mathbf{t}}$ vanishes on the element interior, and arguing as above, is therefore identically zero.

The proof is concluded by observing that the number of functions defined in Table II coincides with the dimension, $(p+1)(p+2)(p+3)/6$, of the space $\mathbb{P}_p$. □

Sets of basis functions similar to those given in Table II are well-known in the literature. For instance, the basis presented in Reference [6] differ only in the choice of local parametrization used to define the basis functions associated with the faces and interior.

3.1.2. Global basis functions. A global basis function φ defined on a physical element $\mathbf{t} \in \mathscr{T}$ is constructed from the basis function $\hat{\varphi}$ defined on the reference element using the standard pull-back transformation:

$$\varphi|_{\mathbf{t}} = \hat{\varphi} \circ \mathbf{F}_{\mathbf{t}}^{-1} \tag{13}$$

The global discrete $L_2(\Omega)$ space of order p is given by

$$X_{p,\mathscr{T}}^{L_2} = \bigoplus_{\mathbf{t}\in\mathscr{T}} \operatorname{span}\{\varphi_{\ell,m,n}^{\mathbf{t}} : 0 \leqslant \ell, m, n \leqslant p\}$$

while the corresponding $H^1(\Omega)$ space is defined by

$$\begin{aligned} X_{p,\mathscr{T}}^{H^1} = & \bigoplus_{\mathbf{v}\in\mathscr{V}} \operatorname{span}\{\varphi^{\mathbf{v}}\} \\ & \bigoplus_{\mathbf{e}\in\mathscr{E}} \operatorname{span}\{\varphi_{\ell}^{\mathbf{e}} : 0 \leqslant \ell \leqslant p-2\} \\ & \bigoplus_{\mathbf{f}\in\mathscr{F}} \operatorname{span}\{\varphi_{\ell,m}^{\mathbf{f}} : 0 \leqslant \ell, m \leqslant p-3\} \\ & \bigoplus_{\mathbf{t}\in\mathscr{T}} \operatorname{span}\{\varphi_{\ell,m,n}^{\mathbf{t}} : 0 \leqslant \ell, m, n \leqslant p-4\} \end{aligned}$$

The next result shows that these are conforming subspaces:

Theorem 3
The spaces $X_{p,\mathscr{T}}^{L_2}$ and $X_{p,\mathscr{T}}^{H^1}$ are L_2-conforming and H^1-conforming subspaces of order p, respectively.

Proof
The case of the space L_2 is trivial since no conformity conditions are required, so restrict attention to the space H^1. Lemma 2 shows that $\hat{X}_{p,\mathscr{T}}^{H^1}$ corresponds to an order p space and it suffices to demonstrate H^1-conformity.

Let $\mathbf{t}$, $\mathbf{t}' \in \mathscr{T}$ be distinct, intersecting tetrahedra. There are three cases to be considered:

Case (i): If $\mathbf{t} \cap \mathbf{t}'$ is a single common vertex $\mathbf{v}$, then the only basis function that is non-zero on both elements is the vertex function $\varphi^{\mathbf{v}} = \lambda_{\mathbf{v}}$, which, being a barycentric coordinate function, is globally continuous.

Case (ii): If $\mathbf{t} \cap \mathbf{t}'$ is a single common edge $\mathbf{e} = [o\ i]$, then, apart from the vertex functions, the edge functions $\varphi_{\ell}^{\mathbf{e}}$ are non-zero on both elements. The restriction of the edge basis function to each element is given by $\beta_{oi}\psi(\xi_{oi})$. Since both $\beta_{oi} = \lambda_o\lambda_i$ and $\xi_{oi} = \lambda_i - \lambda_o$ are globally continuous and depend only on the vertex numbers of the edge, it follows that the edge function is continuous across interfaces between all elements containing the edge.

Case (iii): If $\mathbf{t} \cap \mathbf{t}'$ is a single common face $\mathbf{f} = [o\ i\ j]$, then apart from the vertex and edge functions (already shown to be continuous), the face functions $\varphi^{\mathbf{f}}_{\ell m}$ are non-zero on both elements. The restriction of the face function to both elements is given by $\beta_{oij}\psi_\ell(\xi_{oi})\psi_m(\xi_{oj})$, and, arguing as before, these are smooth functions of the globally continuous barycentric coordinate functions. Thus, the face functions are continuous across the shared interface.

The interior functions are supported on a single element, and are therefore trivially seen to be globally continuous. □

3.2. **H**(**curl**)-*conforming basis functions*

A conforming discretization of the space **H**(**curl**) is characterized by continuity of tangential components across element interfaces. More precisely, Nédélec [9, Lemma 3] shows that if domains K and K' share a common face **f** with normal **n**, then a smooth vector field **u** on each domain belongs to $\mathbf{H}(\mathbf{curl}; K \cup K')$ provided that $\mathbf{n} \wedge \mathbf{u}$ is the same on each side of the face **f**.

3.2.1. Reference element basis functions. The vector-valued polynomial space of order p on the reference element $\hat{\mathbf{t}}$ is given by

$$\hat{\mathbf{X}}^{\mathbf{curl}}_p = (\mathbb{P}_p(\hat{\mathbf{t}}))^3$$

A set of hierarchic basis functions for $\hat{\mathbf{X}}^{\mathbf{curl}}_p$ is given in Table III.

The lowest order edge function $\hat{\boldsymbol{\varphi}}^{\mathbf{e}}_0$ defined in Table III coincides with the so-called Whitney element [1, 14]. The two lowest order edge functions have the property that on an edge $\mathbf{e}'$,

$$\hat{\boldsymbol{\tau}}_{\mathbf{e}} \cdot \hat{\boldsymbol{\varphi}}^{\mathbf{e}}_0|_{\mathbf{e}'} = \begin{cases} 1 & \text{if } \mathbf{e} = \mathbf{e}' \\ 0 & \text{otherwise} \end{cases} \quad \text{and} \quad \hat{\boldsymbol{\tau}}_{\mathbf{e}} \cdot \hat{\boldsymbol{\varphi}}^{\mathbf{e}}_1|_{\mathbf{e}'} = \begin{cases} \xi_{\mathbf{e}} & \text{if } \mathbf{e} = \mathbf{e}' \\ 0 & \text{otherwise} \end{cases}$$

These relations may be generalized by using the recurrence relation (10) defining the Legendre polynomials to reveal that the edge functions defined in Table III satisfy, for $\ell = 0, 1, 2, \ldots$,

$$\hat{\boldsymbol{\tau}}_{\mathbf{e}} \cdot \hat{\boldsymbol{\varphi}}^{\mathbf{e}}_\ell|_{\mathbf{e}'} = \begin{cases} L_\ell(\xi_{\mathbf{e}}) & \text{if } \mathbf{e} = \mathbf{e}' \\ 0 & \text{otherwise} \end{cases} \tag{14}$$

Altogether, there are $(p+1)$ edge basis functions associated with each edge of the reference element, giving $6(p+1)$ in total.

The face functions are more complicated and fall into two categories: *Edge-based face functions* $\hat{\boldsymbol{\varphi}}^{\mathbf{f}}_{\mathbf{e},\ell}$ are associated with the edges **e** of face **f** while *face bubble functions* are associated with the face **f** itself. The key distinction is that face bubble functions on **f** vanish on all other faces while edge-based face functions are also non-zero on the face $\mathbf{f}'$ sharing an edge **e** with **f**. However, since the vector $\hat{\boldsymbol{\nabla}}\hat{\lambda}_{\mathbf{f}\setminus\mathbf{e}}$ is normal to the face $\mathbf{f}'$, the tangential components of $\hat{\boldsymbol{\varphi}}^{\mathbf{f}}_{\mathbf{e},\ell}$ are non-zero only on the face **f** itself. The conformity conditions characterising the space **H**(**curl**) depend only on tangential components and therefore, the degrees of freedom for the edge-based face functions are associated with a single face. This justifies classifying these as *face* functions.

Table III. Hierarchic basis functions for **H**(**curl**)-conforming finite element space of order p.

Space: $(\mathbb{P}_p(\hat{\mathbf{t}}))^3,\ p \in \mathbb{N}$

Edge functions: $\mathbf{e} = [o\ \ i] \in \mathscr{E}(\hat{\mathbf{t}})$

$$\hat{\boldsymbol{\varphi}}^{\mathbf{e}}_0 = \hat{\lambda}_i \hat{\boldsymbol{\nabla}} \hat{\lambda}_o - \hat{\lambda}_o \hat{\boldsymbol{\nabla}} \hat{\lambda}_i$$

$$\hat{\boldsymbol{\varphi}}^{\mathbf{e}}_1 = \hat{\lambda}_i \hat{\boldsymbol{\nabla}} \hat{\lambda}_o + \hat{\lambda}_o \hat{\boldsymbol{\nabla}} \hat{\lambda}_i$$

$$\hat{\boldsymbol{\varphi}}^{\mathbf{e}}_{\ell+1} = \frac{2\ell+1}{\ell+1} L_\ell(\hat{\xi}_{oi}) \hat{\boldsymbol{\varphi}}^{\mathbf{e}}_1 - \frac{\ell}{\ell+1} L_{\ell-1}(\hat{\xi}_{oi}) \hat{\boldsymbol{\varphi}}^{\mathbf{e}}_0, \quad 2 \leqslant \ell \leqslant p-1$$

Edge-based face functions: $\mathbf{f} \in \mathscr{F}(\hat{\mathbf{t}})$

For each edge $\mathbf{e} \subset \partial \mathbf{f}$:

$$\hat{\boldsymbol{\varphi}}^{\mathbf{f}}_{\mathbf{e},\ell} = \beta_{\mathbf{e}} \psi_\ell(\hat{\xi}_{\mathbf{e}}) \hat{\boldsymbol{\nabla}} \hat{\lambda}_{\mathbf{f}\setminus\mathbf{e}}, \quad 0 \leqslant \ell \leqslant p-2$$

where $\mathbf{f}\setminus\mathbf{e}$ denotes the vertex opposite edge $\mathbf{e}$ in face $\mathbf{f}$.

Face bubble functions: $\mathbf{f} = [o\ \ i\ \ j] \in \mathscr{F}(\hat{\mathbf{t}})$

$$\left.\begin{aligned} \hat{\boldsymbol{\varphi}}^{\mathbf{f}}_{i,\ell m} &= \beta_{oij} \psi_\ell(\hat{\xi}_{oi}) \psi_m(\hat{\xi}_{oj}) \hat{\boldsymbol{\tau}}^{[o\ \ i]} \\ \hat{\boldsymbol{\varphi}}^{\mathbf{f}}_{j,\ell m} &= \beta_{oij} \psi_\ell(\hat{\xi}_{oi}) \psi_m(\hat{\xi}_{oj}) \hat{\boldsymbol{\tau}}^{[o\ \ j]} \end{aligned}\right\} \quad 0 \leqslant \ell, m, \ell+m \leqslant p-3$$

Face-based interior functions: $\mathbf{f} = [o\ \ i\ \ j] \in \mathscr{F}(\hat{\mathbf{t}})$

$$\hat{\boldsymbol{\varphi}}^{\hat{\mathbf{t}}}_{\mathbf{f},\ell m} = \beta_{\mathbf{f}} \psi_\ell(\hat{\xi}_{oi}) \psi_m(\hat{\xi}_{oj}) \hat{\boldsymbol{\nabla}} \hat{\lambda}_{\mathbf{t}\setminus\mathbf{f}}, \quad 0 \leqslant \ell, m, \ell+m \leqslant p-3$$

where $\mathbf{t}\setminus\mathbf{f}$ denotes the vertex of $\hat{\mathbf{t}}$ opposite face $\mathbf{f}$.

Interior bubble functions: $\hat{\mathbf{t}} = [o\ \ i\ \ j\ \ k]$

$$\hat{\boldsymbol{\varphi}}^{\hat{\mathbf{t}}}_{d,\ell mn} = \beta_{\mathbf{t}} \psi_\ell(\hat{\xi}_{oi}) \psi_m(\hat{\xi}_{oj}) \psi_n(\hat{\xi}_{ok}) \hat{\mathbf{e}}_d, \quad d \in \{1,2,3\}$$
$$0 \leqslant \ell, m, n, \ell+m+n \leqslant p-4$$

The tangential components of the edge-based functions on face $\mathbf{f}$ satisfy

$$\mathbf{n}^{\mathbf{f}} \wedge \hat{\boldsymbol{\varphi}}^{\mathbf{f}}_{\mathbf{e},\ell}|_{\mathbf{f}} = c \beta_{\mathbf{e}} \psi_\ell(\xi_{\mathbf{e}}) \boldsymbol{\tau}_{\mathbf{e}} \tag{15}$$

which follows from the observation that

$$\mathbf{n}^{\mathbf{f}} \wedge \hat{\boldsymbol{\nabla}} \hat{\lambda}_{\mathbf{f}\setminus\mathbf{e}} = c \boldsymbol{\tau}_{\mathbf{e}}$$

where c is the (non-zero) determinant of the matrix whose columns are formed from the components of the constant vectors $\boldsymbol{\tau}_{\mathbf{e}}$, $\mathbf{n}^{\mathbf{f}}$ and $\hat{\boldsymbol{\nabla}} \hat{\lambda}_{\mathbf{f}\setminus\mathbf{e}}$. Altogether, there are $3(p-1)$ edge-based face functions and $(p-1)(p-2)$ face bubble functions for each face of the reference tetrahedron, giving $4(p-1)(p+1)$ face functions in total.

The interior functions also fall into two categories: *Interior bubble functions* vanish on all faces of the tetrahedron while *face-based interior functions* are non-zero on certain faces. However, the tangential components of the face-based functions do vanish on all faces of the tetrahedron. Nevertheless, the classification as *interior functions* is justified since

H(**curl**)-conformity imposes conditions on tangential components only, meaning that the coefficients of the face-based functions can be chosen independently on each element.

There are $(p-1)(p-2)(p-3)/2$ interior bubble functions and $(p-1)(p-2)/2$ face-based interior functions for each face of the reference element, giving $(p-1)(p-2)(p+1)/2$ in total.

Lemma 4
The set of functions defined in Table III forms a hierarchic basis for the spaces $\hat{\mathbf{X}}_p^{\mathbf{curl}}$, $p \in \mathbb{N}$.

Proof
Observe that each of the functions defined in Table III belongs to the space $(\mathbb{P}_p)^3$. The next step is to show the functions are linearly independent. Suppose that

$$\sum_{\mathbf{e}\in\mathscr{E}} \mathbf{w}^{\mathbf{e}} + \sum_{\mathbf{f}} \sum_{\mathbf{e}\subset\partial\mathbf{f}} \mathbf{w}_{\mathbf{e}}^{\mathbf{f}} + \sum_{\mathbf{f}} \mathbf{w}^{\mathbf{f}} + \sum_{\mathbf{f}} \mathbf{w}_{\mathbf{f}}^{\mathbf{t}} + \mathbf{w}^{\mathbf{t}} \equiv \mathbf{0} \tag{16}$$

where $\mathbf{w}^{\mathbf{e}}$, $\mathbf{w}^{\mathbf{f}}$, $\mathbf{w}_{\mathbf{e}}^{\mathbf{f}}$, $\mathbf{w}_{\mathbf{f}}^{\mathbf{t}}$ and $\mathbf{w}^{\mathbf{t}}$ are linear combinations of edge, face and interior functions, respectively. With the aid of Lemma 1, it is not difficult to show that the basis functions within these categories are linearly independent, and it therefore suffices to show (16) implies the each of the above functions must vanish individually.

Let $\mathbf{e} \in \mathscr{E}$ be any edge, then, taking inner product of (16) with $\boldsymbol{\tau}_{\mathbf{e}}$ on the edge gives

$$\boldsymbol{\tau}_{\mathbf{e}} \cdot \mathbf{w}^{\mathbf{e}}|_{\mathbf{e}} = 0$$

since the tangential components of the face and interior functions vanish on all edges. Property (14) then implies that $\mathbf{w}^{\mathbf{e}} = \mathbf{0}$ and it follows that the first term in (16) vanishes.

Let $\mathbf{f} \in \mathscr{F}$ be a face containing the edge $\mathbf{e}$, then, forming the vector product of (16) with $\mathbf{n}^{\mathbf{f}}$ on the face $\mathbf{f}$ gives

$$\mathbf{n}^{\mathbf{f}} \wedge \mathbf{w}_{\mathbf{e}}^{\mathbf{f}}|_{\mathbf{f}} + \mathbf{n}^{\mathbf{f}} \wedge \mathbf{w}^{\mathbf{f}}|_{\mathbf{f}} = \mathbf{0} \tag{17}$$

since the tangential components of interior functions and the face bubble functions vanish on all faces. Restricting (17) to an edge of face $\mathbf{f}$ and recalling the face bubble functions vanish on the edges, and then applying property (15) shows that the edge-based face function $\mathbf{w}_{\mathbf{e}}^{\mathbf{f}} = \mathbf{0}$ and it follows that the second term in (16) must vanish. Equation (17) then implies the third term vanishes too.

Similarly, taking inner products of (16) with $\mathbf{n}^{\mathbf{f}}$ on the face $\mathbf{f}$ gives

$$\mathbf{n}^{\mathbf{f}} \cdot \mathbf{w}_{\mathbf{f}}^{\mathbf{t}}|_{\mathbf{f}} = 0$$

since the interior bubble functions vanish on all faces. Inserting the expressions for the face-based interior functions and noting that the gradient is normal to the face leads to the conclusion $\mathbf{w}_{\mathbf{f}}^{\mathbf{t}} = \mathbf{0}$ and the third term in Equation (16) drops out. Consequently, Equation (16) reduces to $\mathbf{w}^{\mathbf{t}} = \mathbf{0}$ and it follows that the basis functions are linearly independent.

The proof is concluded by observing that the number of basis functions defined in Table III coincides with the dimension, $(p+1)(p+2)(p+3)/2$, of the space $(\mathbb{P}_p)^3$. □

3.2.2. Global basis functions. A global basis function $\boldsymbol{\varphi}$ of **H**(**curl**) defined on a physical element $\mathbf{t} \in \mathscr{T}$ is constructed from the basis function $\hat{\boldsymbol{\varphi}}$ defined on the reference element using

a covariant transformation:

$$\varphi|_{\mathbf{t}} = (\mathbf{J}_{\mathbf{t}}^{-\top}\hat{\boldsymbol{\varphi}}) \circ \mathbf{F}_{\mathbf{t}}^{-1} \tag{18}$$

The global discrete $\mathbf{H}(\mathbf{curl})$ space of order p is defined by

$$\begin{aligned}
\mathbf{X}_{p,\mathscr{T}}^{\mathbf{curl}} = & \bigoplus_{\mathbf{e}\in\mathscr{E}} \operatorname{span}\{\boldsymbol{\varphi}_{\ell}^{\mathbf{e}} : 0 \leqslant \ell \leqslant p\} \\
& \bigoplus_{\mathbf{f}\in\mathscr{F}} \operatorname{span}\{\boldsymbol{\varphi}_{\mathbf{e},\ell}^{\mathbf{f}} : 0 \leqslant \ell \leqslant p-2, \mathbf{e} \subset \partial\mathbf{f}\} \\
& \bigoplus_{\mathbf{f}=[o\ \ i\ \ j]\in\mathscr{F}} \operatorname{span}\{\boldsymbol{\varphi}_{i,\ell m}^{\mathbf{f}}, \boldsymbol{\varphi}_{j,\ell m}^{\mathbf{f}} : 0 \leqslant \ell, m \leqslant p-3\} \\
& \bigoplus_{\mathbf{t}\in\mathscr{T}} \operatorname{span}\{\boldsymbol{\varphi}_{\mathbf{f},\ell m}^{\mathbf{t}} : 0 \leqslant \ell, m \leqslant p-3, \mathbf{f} \subset \partial\mathbf{t}\} \\
& \bigoplus_{\mathbf{t}\in\mathscr{T}} \operatorname{span}\{\boldsymbol{\varphi}_{d,\ell mn}^{\mathbf{t}} :\ d \in \{1,2,3\}, 0 \leqslant \ell, m, n \leqslant p-4\}
\end{aligned}$$

The main result of this section reads as follows:

Theorem 5
The space $\mathbf{X}_{p,\mathscr{T}}^{\mathbf{curl}}$ is an $\mathbf{H}(\mathbf{curl})$-conforming subspace of order p.

Proof
Let $p \in \mathbb{N}$ be fixed. Lemma 4 shows that the space is of pth order. It only remains to show that if distinct elements $\mathbf{t}$ and $\mathbf{t}'$ share a common face $\mathbf{f}$, then for each global basis function, the quantity $\mathbf{n}^{\mathbf{f}} \wedge \boldsymbol{\varphi}$ is continuous across the face $\mathbf{f}$.
Edge functions: Let $\mathbf{e} \subset \partial\mathbf{f}$ be an edge of the shared face. The higher order edge functions $\hat{\boldsymbol{\varphi}}_{\ell}^{\mathbf{e}}$ are combinations of functions of $\xi_{\mathbf{e}}$ multiplied by the two lowest order edge functions, which, in turn, are combinations of the gradients of the barycentric co-ordinates on the edge. The co-ordinate $\xi_{\mathbf{e}}$ is continuous on the shared face, and it therefore suffices to show that $\mathbf{n}^{\mathbf{f}} \wedge \mathbf{J}_t^{-\top}\hat{\boldsymbol{\nabla}}\hat{\lambda}$ is continuous across the face, where $\hat{\lambda}$ is a barycentric co-ordinate on the face. The chain rule confirms that $\mathbf{J}_t^{-\top}\hat{\boldsymbol{\nabla}}\hat{\lambda}$ is simply the gradient with respect to the physical co-ordinates, $\boldsymbol{\nabla}\lambda$. The barycentric coordinate functions have continuous tangential components across shared faces, and therefore $\mathbf{n}^{\mathbf{f}} \wedge \boldsymbol{\nabla}\lambda$ is continuous across the interface.
Face functions: The tangential components of both types of face function are only non-zero on the face $\mathbf{f}$ with which they are associated. On the face, the edge-based face functions are combinations of functions of the barycentric co-ordinates on the face and their gradients. Consequently, arguing as in the case of edge functions, we conclude that the tangential components are continuous across the interface. The face bubble functions are also functions of the barycentric coordinates on the face and the two intrinsic tangent vectors $\boldsymbol{\tau}_i^{\mathbf{f}}$, $\boldsymbol{\tau}_j^{\mathbf{f}}$ defined on the face. Consequently, since the tangent vectors coincide on the elements sharing the interface, it follows that the face bubble functions are $\mathbf{H}(\mathbf{curl})$-conforming.
Interior functions: Both types of face function have vanishing tangential components on all faces, and are therefore trivially seen to be conforming. □

Table IV. Hierarchic basis functions for **H**(**div**)-conforming finite element space of order p.

Space: $(\mathbb{P}_p(\hat{\mathbf{t}}))^3,\ p \in \mathbb{N}$

Edge-based face functions: $\mathbf{f} \in \mathscr{F}(\hat{\mathbf{t}})$
For each edge $\mathbf{e} = [o\ i] \subset \partial\mathbf{f}$:

$$\hat{\boldsymbol{\varphi}}^{\mathbf{f}}_{\mathbf{e},\ell} = \psi_\ell(\xi_{\mathbf{e}})\hat{\boldsymbol{\varphi}}^{\mathbf{f}}_{\mathbf{e}}, \quad 0 \leqslant \ell \leqslant p-1$$

where

$$\hat{\boldsymbol{\varphi}}^{\mathbf{f}}_{\mathbf{e}} = \hat{\lambda}_{\mathbf{f}\backslash\mathbf{e}}\hat{\boldsymbol{\nabla}}\hat{\lambda}_o \wedge \hat{\boldsymbol{\nabla}}\hat{\lambda}_i$$

and $\mathbf{f}\backslash\mathbf{e}$ denotes the vertex opposite edge $\mathbf{e}$ in face $\mathbf{f}$.

Face bubble functions: $\mathbf{f} = [o\ i\ j] \in \mathscr{F}(\hat{\mathbf{t}})$

$$\hat{\boldsymbol{\varphi}}^{\mathbf{f}}_{\ell m} = \beta_{oij}\psi_\ell(\hat{\xi}_{oi})\psi_m(\hat{\xi}_{oj})\hat{\boldsymbol{\nabla}}\hat{\lambda}_i \wedge \hat{\boldsymbol{\nabla}}\hat{\lambda}_j, \quad 0 \leqslant \ell, m, \ell+m \leqslant p-3$$

Edge-based interior functions: $\mathbf{e} \in \mathscr{E}(\hat{\mathbf{t}})$

$$\hat{\boldsymbol{\varphi}}^{\hat{\mathbf{t}}}_{\mathbf{e},\ell} = \beta_{\mathbf{e}}\psi_\ell(\hat{\xi}_{oi})\hat{\boldsymbol{\tau}}^{\mathbf{e}}, \quad 0 \leqslant \ell \leqslant p-2$$

Face-based interior functions: $\mathbf{f} = [o\ i\ j] \in \mathscr{F}(\hat{\mathbf{t}})$

$$\left.\begin{aligned}\hat{\boldsymbol{\varphi}}^{\hat{\mathbf{t}}}_{\mathbf{f},i,\ell m} &= \beta_{oij}\psi_\ell(\hat{\xi}_{oi})\psi_m(\hat{\xi}_{oj})\hat{\boldsymbol{\tau}}^{[o\ \ i]}\\ \hat{\boldsymbol{\varphi}}^{\hat{\mathbf{t}}}_{\mathbf{f},j,\ell m} &= \beta_{oij}\psi_\ell(\hat{\xi}_{oi})\psi_m(\hat{\xi}_{oj})\hat{\boldsymbol{\tau}}^{[o\ \ j]}\end{aligned}\right\} \quad 0 \leqslant \ell, m, \ell+m \leqslant p-3$$

Interior bubble functions: $\hat{\mathbf{t}} = [o\ i\ j\ k]$

$$\hat{\boldsymbol{\varphi}}^{\hat{\mathbf{t}}}_{d,\ell mn} = \beta_{\mathbf{t}}\psi_\ell(\hat{\xi}_{oi})\psi_m(\hat{\xi}_{oj})\psi_n(\hat{\xi}_{ok})\hat{\mathbf{e}}_d, \quad d \in \{1,2,3\}$$
$$0 \leqslant \ell, m, n, \ell+m+n \leqslant p-4$$

3.3. **H**(**div**)-*conforming basis functions*

A conforming discretization of the space **H**(**div**) is characterized by the continuity of the normal components across element interfaces. More precisely, Nédélec [9, Lemma 1] shows that if domains K and K' share a common face $\mathbf{f}$ with normal $\mathbf{n}$, then a smooth vector field $\mathbf{u}$ on each domain belongs to $\mathbf{H}(\mathbf{div}; K \cup K')$ provided that $\mathbf{n} \cdot \mathbf{u}$ is the same on each side of the face $\mathbf{f}$.

3.3.1. Reference element basis functions. The vector-valued polynomial space of order p on the reference element $\hat{\mathbf{t}}$ is given by

$$\hat{\mathbf{X}}^{\mathbf{div}}_p = (\mathbb{P}_p(\hat{\mathbf{t}}))^3$$

A set of hierarchic basis functions for $\hat{\mathbf{X}}^{\mathbf{div}}_p$ is given in Table IV.

The edge-based face functions defined in Table IV associated with each edge $\mathbf{e} = [o\ i]$ of face $\mathbf{f}$, are linear combinations of the elementary functions

$$\hat{\boldsymbol{\varphi}}^{\mathbf{f}}_{\mathbf{e}} = \hat{\lambda}_{\mathbf{f}\backslash\mathbf{e}}\hat{\boldsymbol{\nabla}}\hat{\lambda}_o \wedge \hat{\boldsymbol{\nabla}}\hat{\lambda}_i$$

where $\mathbf{f}\backslash\mathbf{e}$ denotes the vertex opposite edge $\mathbf{e}$ in face $\mathbf{f}$. These functions are used in Reference [7] to construct a basis for the lowest order, or Whitney, elements in the form

$$2\sum_{\mathbf{e}\subset\partial\mathbf{f}}\hat{\boldsymbol{\varphi}}_{\mathbf{e}}^{\mathbf{f}}$$

It is not difficult to verify that the normal component of the function $\hat{\boldsymbol{\varphi}}_{\mathbf{e}}^{\mathbf{f}}$ on a face $\mathbf{f}'$ vanishes unless $\mathbf{f}'$ and $\mathbf{f}$ coincide,

$$\mathbf{n}^{\mathbf{f}'}\cdot\hat{\boldsymbol{\varphi}}_{\mathbf{e}}^{\mathbf{f}}=0,\quad \mathbf{f}\neq\mathbf{f}'$$

There are p edge-based face functions associated with each of the three edges of face $\mathbf{f}$, giving in total $12p$ functions on the tetrahedron.

The normal component of the face bubble functions vanishes on all edges and on all faces except the face with which they are associated. There are $(p-2)(p-1)/2$ functions per face, and consequently $2(p-2)(p-1)$ face bubble functions altogether on the tetrahedron.

There are three types of interior function. The normal components of all types of interior function vanish on all faces of the tetrahedron. The edge-based interior functions have non-zero tangential components on the edge with which they are associated and account for $6(p-1)$ basis functions in total. The face-based interior functions have vanishing tangential components on all edges, but have non-zero tangential components on the face with which they are associated. These account for $2(p-1)(p-2)$ basis functions. Finally, the interior bubble functions vanish on all boundaries and account for $(p-3)(p-2)(p-1)/2$ functions in total.

These observations are used to prove the following result:

Lemma 6
The set of functions defined in Table IV forms a hierarchic basis for the spaces $\hat{\mathbf{X}}_p^{\mathbf{div}}$, $p\in\mathbb{N}$.

Proof
Each of the functions defined in Table IV belongs to the space $(\mathbb{P}_p)^3$. The next step is to show the functions are linearly independent. Suppose that

$$\sum_{\mathbf{f}}\sum_{\mathbf{e}\subset\partial\mathbf{f}}\mathbf{w}_{\mathbf{e}}^{\mathbf{f}}+\sum_{\mathbf{f}}\mathbf{w}^{\mathbf{f}}+\sum_{\mathbf{e}\in\mathscr{E}}\mathbf{w}_{\mathbf{e}}^{\mathbf{t}}+\sum_{\mathbf{f}}\mathbf{w}_{\mathbf{f}}^{\mathbf{t}}+\mathbf{w}^{\mathbf{t}}\equiv\mathbf{0}\tag{19}$$

where $\mathbf{w}_{\mathbf{e}}^{\mathbf{f}}$, $\mathbf{w}^{\mathbf{f}}$, $\mathbf{w}_{\mathbf{e}}^{\mathbf{t}}$, $\mathbf{w}_{\mathbf{f}}^{\mathbf{t}}$ and $\mathbf{w}^{\mathbf{t}}$ are linear combinations of face and interior functions respectively. The basis functions within these categories are linearly independent, and it therefore suffices to show (19) implies the each of the above functions must vanish individually.

Taking inner products of (19) with $\mathbf{n}^{\mathbf{f}}$ and evaluating on a face $\mathbf{f}\in\mathscr{F}$ gives

$$\sum_{\mathbf{e}\subset\partial\mathbf{f}}\mathbf{n}^{\mathbf{f}}\cdot\mathbf{w}_{\mathbf{e}}^{\mathbf{f}}|_{\mathbf{f}}+\mathbf{n}^{\mathbf{f}}\cdot\mathbf{w}^{\mathbf{f}}|_{\mathbf{f}}=0$$

since the normal components of the interior functions vanish on all faces. Recalling that the face bubble functions vanish on all edges and using properties of the edge-based face functions reveals firstly that $\mathbf{w}_{\mathbf{e}}^{\mathbf{f}}=\mathbf{0}$, and hence that $\mathbf{w}^{\mathbf{f}}=\mathbf{0}$.

Consequently, the first two terms in (19) vanish. The remaining terms vanish too. Firstly, the edge-based interior functions are the only non-zero functions on the edges and must therefore be zero. Then, the face-based interior functions are the only remaining non-zero functions

on the faces and must also vanish identically. Thus, Equation (19) reduces to $\mathbf{w}^{\mathbf{t}} = \mathbf{0}$ and it follows that the basis functions are linearly independent.

The proof is concluded by observing that the number of basis functions defined in Table IV coincides with the dimension, $(p+1)(p+2)(p+3)/2$, of the space $(\mathbb{P}_p)^3$. □

3.3.2. Global basis functions. A global basis function $\boldsymbol{\varphi}$ of $\mathbf{H}(\mathbf{div})$ defined on a physical element $\mathbf{t} \in \mathscr{T}$ is constructed from the basis function $\hat{\boldsymbol{\varphi}}$ defined on the reference element using the contravariant (Piola) transformation [34]:

$$\varphi|_{\mathbf{t}} = \frac{1}{\det(\mathbf{J}_{\mathbf{t}})}(\mathbf{J}_{\mathbf{t}}\hat{\boldsymbol{\varphi}}) \circ \mathbf{F}_{\mathbf{t}}^{-1} \tag{20}$$

The Piola transformation has the follow important property

$$\frac{1}{\det(\mathbf{J}_{\mathbf{t}})}\,\mathbf{J}_{\mathbf{t}}(\hat{\boldsymbol{\nabla}}\hat{\lambda}_o \wedge \hat{\boldsymbol{\nabla}}\hat{\lambda}_i) = \boldsymbol{\nabla}\lambda_o \wedge \boldsymbol{\nabla}\lambda_i \tag{21}$$

The global discrete $\mathbf{H}(\mathbf{div})$ space of order p is defined by

$$\begin{aligned}
\mathbf{X}^{\mathbf{div}}_{p,\mathscr{T}} = & \bigoplus_{\mathbf{f}\in\mathscr{F}} \operatorname{span}\{\boldsymbol{\varphi}^{\mathbf{f}}_{\mathbf{e},\ell} : 0 \leqslant \ell \leqslant p-1, \mathbf{e} \subset \partial\mathbf{f}\} \\
& \bigoplus_{\mathbf{f}\in\mathscr{F}} \operatorname{span}\{\boldsymbol{\varphi}^{\mathbf{f}}_{\ell m} : 0 \leqslant \ell, m, \ell+m \leqslant p-3\} \\
& \bigoplus_{\mathbf{t}\in\mathscr{T}} \operatorname{span}\{\boldsymbol{\varphi}^{\mathbf{t}}_{\mathbf{e},\ell} : 0 \leqslant \ell \leqslant p-2, \mathbf{e} \subset \partial\mathbf{t}\} \\
& \bigoplus_{\mathbf{t}\in\mathscr{T}} \operatorname{span}\{\boldsymbol{\varphi}^{\mathbf{t}}_{\mathbf{f},i,\ell m}, \boldsymbol{\varphi}^{\mathbf{t}}_{\mathbf{f},j,\ell m} : 0 \leqslant \ell, m \leqslant p-3, \mathbf{f} = [o\ \ i\ \ j] \in \mathscr{F}(\mathbf{t})\} \\
& \bigoplus_{\mathbf{t}\in\mathscr{T}} \operatorname{span}\{\boldsymbol{\varphi}^{\mathbf{t}}_{d,\ell mn} : d \in \{1,2,3\}, 0 \leqslant \ell, m, n \leqslant p-4\}
\end{aligned}$$

This constitutes an $\mathbf{H}(\mathbf{div})$-conforming basis:

Theorem 7
The space $\mathbf{X}^{\mathbf{div}}_{p,\mathscr{T}}$ is an $\mathbf{H}(\mathbf{div})$-conforming subspace of order p.

Proof
Fix $p \in \mathbb{N}$. Lemma 6 shows that the space is of pth order and it suffices to show that if distinct elements $\mathbf{t}$ and $\mathbf{t}'$ share a common face $\mathbf{f}$, then for each global basis function, the quantity $\mathbf{n}^{\mathbf{f}} \cdot \boldsymbol{\varphi}$ is continuous across the face $\mathbf{f}$.
Interior functions: All types of face function have vanishing normal components on all faces, and are therefore $\mathbf{H}(\mathbf{div})$-conforming.
Face functions: Let $\mathbf{e} = [o\ \ i] \subset \partial\mathbf{f}$ be an edge of the shared face. The face functions are combinations of functions of $\xi_{\mathbf{e}}$ multiplied by the images of products of the form $\hat{\boldsymbol{\nabla}}\hat{\lambda}_i \wedge \hat{\boldsymbol{\nabla}}\hat{\lambda}_j$ under the Piola transformation, which, in view of relation (21) are given by $\boldsymbol{\nabla}\lambda_i \wedge \boldsymbol{\nabla}\lambda_j$. The co-ordinate $\xi_{\mathbf{e}}$ is continuous on the shared face, and it suffices to show that the normal component of $\boldsymbol{\nabla}\lambda_i \wedge \boldsymbol{\nabla}\lambda_j$ is continuous across the face. This quantity only depends on the tangential

components of $\nabla\lambda_o$ and $\nabla\lambda_i$ on $\mathbf{f}$. However, the barycentric co-ordinates are continuous and thus the tangential components of their gradients is continuous across a face and it follows that the normal components of the face functions match across a face. □

4. IMPLEMENTATION

The application of the basis functions to the situation where elements of non-uniform local polynomial order are required is now considered. The generalization to non-uniform order is straightforward provided a hierarchical basis is available once it is realized [35], that one only need construct the *connectivity mappings*.

Connectivity mappings play a key role in finite element analysis. For instance, they are used to distribute the global solution vector to the elements and in the assembly of the global linear system. The standard finite element sub-assembly procedure for a global matrix $\mathbf{M}$, such as the mass matrix, may be written in the form [35, 36]

$$\mathbf{M} = \sum_{\mathbf{t}\in\mathscr{T}} \mathbf{\Lambda}_{\mathbf{t}}\mathbf{M}_{\mathbf{t}}\mathbf{\Lambda}_{\mathbf{t}}^{\top} \tag{22}$$

where $\mathbf{M}_{\mathbf{t}}$ are element matrices and $\mathbf{\Lambda}_{\mathbf{t}}$ are connectivity mappings.

A connectivity mapping is represented by a rectangular Boolean matrix of dimension $N \times N_{\mathbf{t}}$ where N is the total number of global degrees of freedom and $N_{\mathbf{t}}$ is the number of degrees of freedom on element $\mathbf{t}$. The entries of the matrix are given by

$$[\mathbf{\Lambda}_{\mathbf{t}}]_{ij} = \begin{cases} 1 & \text{if } i \text{ is the global number of local degree of freedom } j \\ 0 & \text{otherwise} \end{cases} \tag{23}$$

To re-iterate, the construction of the connectivity mappings is the only modification of the standard finite element methodology needed to implement locally non-uniform order approximation. All other operations such as the evaluation of the element matrices, application of boundary conditions, etc. follow the usual approach.

The implementation of the bases for non-uniform local polynomial order will be illustrated by considering a simple mesh comprised of five elements

$$\mathscr{T} = \{\mathbf{t}_1, \ldots, \mathbf{t}_5\}$$

shown in Figure 7. The elements and the desired polynomial orders are given by

$$\begin{aligned} \mathbf{t}_1 &= [2\ 6\ 4\ 8]; \quad p_1 = 5 \\ \mathbf{t}_2 &= [2\ 3\ 6\ 8]; \quad p_2 = 4 \\ \mathbf{t}_3 &= [1\ 4\ 2\ 6]; \quad p_3 = 3 \\ \mathbf{t}_4 &= [2\ 4\ 5\ 8]; \quad p_4 = 2 \\ \mathbf{t}_5 &= [4\ 6\ 7\ 8]; \quad p_5 = 4 \end{aligned} \tag{24}$$

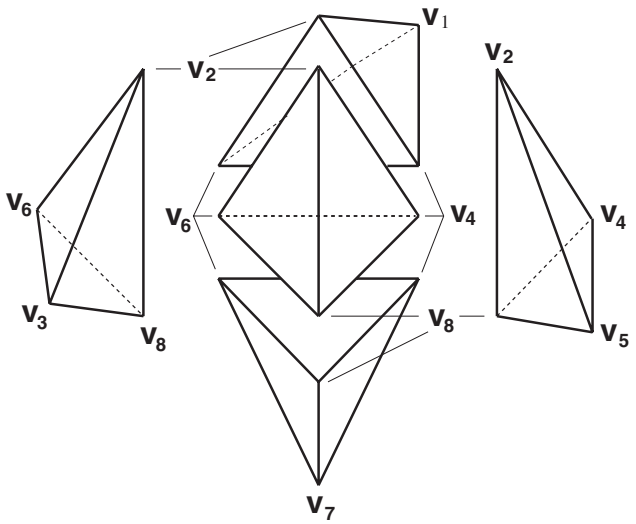

Figure 7. Exploded view of five-element mesh used to illustrate variable order implementation.

where the elements have been oriented as described in the previous section. The first element $\mathbf{t}_1$ represents the most common situation whereby an element has neighbouring elements on all faces. Here, in order to avoid a proliferation of data, only the information needed for element $\mathbf{t}_1$ will be presented in detail, since the treatment of larger numbers of elements follows the same pattern.

The vertices $\mathscr{V}(\mathbf{t}_1)$, edges $\mathbf{E}(\mathbf{t}_1)$ and faces $\mathscr{F}(\mathbf{t}_1)$ of element $\mathbf{t}_1$ are easily identified from the global vertex numbers [2 6 4 8] of the element:

$$\mathscr{V}(\mathbf{t}_1) = \{[2,4,6,8]\}$$

$$\mathscr{E}(\mathbf{t}_1) = \{\mathbf{e}_1, \mathbf{e}_2, \ldots, \mathbf{e}_6\}$$

$$\mathscr{F}(\mathbf{t}_1) = \{\mathbf{f}_1, \mathbf{f}_2, \mathbf{f}_3, \mathbf{f}_4\}$$

where the edges and faces are defined in Table V. The complete sets $\mathscr{V}$, $\mathscr{E}$ and $\mathscr{F}$ of vertices, edges and interiors are compiled by forming the unions of such elemental contributions by looping over elements. At the same time, the active polynomial order applied on each entity is also be determined by applying a *minimum rule* [35]. This rule states that the active order of approximation an edge or face is taken to be the minimum degree of all elements containing the edge or face. For instance, face $\mathbf{f}_1$ is shared by elements $\mathbf{t}_1$ and $\mathbf{t}_2$, having local orders 5 and 4, respectively. Applying the minimum rule gives a local order of approximation $\min(4,5) = 4$ on face $\mathbf{f}_1$. The local order of approximation on edge $\mathbf{e}_1$ is the minimum order of the elements $\mathbf{t}_1$, $\mathbf{t}_2$ and $\mathbf{t}_3$ containing the edge, giving an order $\min(5,4,3) = 3$ on the edge. Table V shows the local orders approximation on all edges and faces of element $\mathbf{t}_1$.

Table V. Edges and faces of element $\mathbf{t}_1$ and local order of approximation determined from using minimum degree of elements containing the entity.

Entity	Vertices	Contained within	Local order
$\mathbf{e}_1$	[2 6]	$\mathbf{t}_1, \mathbf{t}_2, \mathbf{t}_3$	3
$\mathbf{e}_2$	[2 8]	$\mathbf{t}_1, \mathbf{t}_2, \mathbf{t}_4$	2
$\mathbf{e}_3$	[6 8]	$\mathbf{t}_1, \mathbf{t}_2, \mathbf{t}_5$	1
$\mathbf{e}_4$	[2 4]	$\mathbf{t}_1, \mathbf{t}_3, \mathbf{t}_4$	2
$\mathbf{e}_5$	[4 6]	$\mathbf{t}_1, \mathbf{t}_3, \mathbf{t}_5$	1
$\mathbf{e}_6$	[4 8]	$\mathbf{t}_1, \mathbf{t}_4, \mathbf{t}_5$	1
$\mathbf{f}_1$	[2 6 8]	$\mathbf{t}_1, \mathbf{t}_2$	4
$\mathbf{f}_2$	[2 4 6]	$\mathbf{t}_1, \mathbf{t}_3$	3
$\mathbf{f}_3$	[2 4 8]	$\mathbf{t}_1, \mathbf{t}_4$	2
$\mathbf{f}_4$	[4 6 8]	$\mathbf{t}_1, \mathbf{t}_5$	1

Table VI. Number of degrees of freedom $N(\mathbf{c}, p)$ needed on each entity $\mathbf{c}$ (i.e. vertex, edge, face or interior) for the various spaces if the active order of approximation on the entity is $p \in \mathbb{N}$. (Negative quantities correspond to no basis functions.)

Space	Vertices	Edges	Faces	Interiors
H^1	1	$p-1$	$(p-2)(p-1)/2$	$(p-3)(p-2)(p-1)/6$
$\mathbf{H}(\mathbf{curl})$	0	$p+1$	$(p-1)(p+1)$	$(p-2)(p-1)(p+1)/2$
$\mathbf{H}(\mathbf{div})$	0	0	$(p+1)(p+2)/2$	$(p-1)(p+1)(p+2)/2$
L_2	0	0	0	$(p+1)(p+2)(p+3)/6$

Once all vertices, edges, faces and interiors have been identified, global numbers are assigned to the degrees of freedom and the connectivity mapping is constructed. This process is performed as follows:

1. For each entity $\mathbf{c} \in \mathscr{V} \cup \mathscr{E} \cup \mathscr{F} \cup \mathscr{T}$, (i.e. each element vertex, edge, face and interior):
   (a) Find the local order of approximation $p_{\mathbf{c}}$.
   (b) Determine the number of degrees of freedom $N(\mathbf{c}, p_{\mathbf{c}})$ needed on the entity by reference to Table VI.
   (c) Assign global numbers and distribute to all elements containing the entity.
2. For each element $\mathbf{t} \in \mathscr{T}$: Construct the connectivity mapping $\mathbf{\Lambda}_{\mathbf{t}}$.

The following sections detail the construction of the connectivity mappings for the five-element mesh described above.

4.1. L_2-conforming subspace

The basis functions for an L_2-conforming subspace given in Table I consist entirely of interior functions and global numbers are needed only for the interior degrees of freedom, as indicated

in Table VI. The local order of approximation on element $\mathbf{t}_1$ is $p=5$ and Table VI indicates that 56 degrees of freedom are assigned to element $\mathbf{t}_1$.

Suppose that the global numbers $\{116,\ldots,171\}$ are assigned. In theory, the connectivity mapping $\mathbf{\Lambda}_1$ will be a rectangular matrix of size $N \times 56$, where N is the total number of global degrees of freedom with entries defined as in Equation (23). In practice, this matrix is never explicitly constructed, and instead the information is stored in the more compact form

$$\mathbf{\Lambda}_1 = [116 \ \ldots \ 171]$$

The correspondence between the numbers and the particular basis functions is a matter of taste, provided that any scheme is used consistently.

4.2. H^1-conforming subspace

The basis functions for an H^1-conforming subspace given in Table II are separated into subsets of basis functions associated with the individual vertices, edges, faces and element interior. The connectivity mapping on element $\mathbf{t}$ may be decomposed accordingly, giving

$$\mathbf{\Lambda}_\mathbf{t} = \begin{bmatrix} \mathbf{\Lambda}_\mathbf{t}^{\mathscr{V}} & & & & & & & \\ & \mathbf{\Lambda}_\mathbf{t}^{\mathbf{e}_1} & & & & & & \\ & & \ddots & & & & & \\ & & & \mathbf{\Lambda}_\mathbf{t}^{\mathbf{e}_6} & & & & \\ & & & & \mathbf{\Lambda}_\mathbf{t}^{\mathbf{f}_1} & & & \\ & & & & & \ddots & & \\ & & & & & & \mathbf{\Lambda}_\mathbf{t}^{\mathbf{f}_3} & \\ & & & & & & & \mathbf{\Lambda}_\mathbf{t}^{\mathbf{t}} \end{bmatrix}$$

where the remaining entries are zeros, or, more compactly,

$$\mathbf{\Lambda}_\mathbf{t} = \mathtt{blockdiag}[\mathbf{\Lambda}_\mathbf{t}^{\mathscr{V}}, \mathbf{\Lambda}_\mathbf{t}^{\mathbf{e}_1}, \ldots, \mathbf{\Lambda}_\mathbf{t}^{\mathbf{e}_6}, \mathbf{\Lambda}_\mathbf{t}^{\mathbf{f}_1}, \ldots, \mathbf{\Lambda}_\mathbf{t}^{\mathbf{f}_3}, \mathbf{\Lambda}_\mathbf{t}^{\mathbf{t}}] \tag{25}$$

Table VI indicates that one degree of freedom per vertex is needed for the space H^1 giving a total of four for the element. If the actual numbers assigned are selected to coincide with the vertex numbers, then the compact storage scheme described above gives

$$\mathbf{\Lambda}_1^{\mathscr{V}} = [2 \ 4 \ 6 \ 8]$$

Similarly, Table V shows that edge $\mathbf{e}_1$ has local order of approximation $p=3$ and then Table VI indicates that two global numbers, $\{9,10\}$ say, are to be assigned. The local order of element $\mathbf{t}_1$ is $p=5$ meaning that each edge has four basis functions, while only two freedom numbers have been assigned. This is to be expected, since the highest order, $p=4$ and 5, edge functions must have coefficients equal to zero in order to preserve conformity with lower order elements sharing the edge. This is enforced by assigning a global freedom number of '0' to all such degrees of freedom. The contribution to the connectivity mapping for the element from edge $\mathbf{e}_1$ is therefore given by

$$\mathbf{\Lambda}_1^{\mathbf{e}_1} = [9 \ 10 \ 0 \ 0]$$

Equally well, Table V shows that face $\mathbf{f}_1$ has a local order $p=4$ and then Table VI indicates that three global numbers, $\{11, 12, 13\}$ say, are assigned. However, there are six local basis functions on each face of a fifth order element. As described above, the three actual global numbers are padded out with zeros giving

$$\mathbf{\Lambda}_1^{\mathbf{f}_1} = [11 \;\; 12 \;\; 13 \;\; 0 \;\; 0 \;\; 0]$$

This process continues until finally it is observed that four interior degrees of freedom is needed, $\{85, 86, 87, 88\}$ say, giving

$$\mathbf{\Lambda}_1^{\mathbf{t}} = [85 \;\; 86 \;\; 87 \;\; 88]$$

It is then a simple matter to concatenate the connectivity mappings for each entity to form the element connectivity mapping in the form of a string of integers and zeros. The zeros indicate columns of zeros in the full matrix representation and automatically enforce that the coefficients of the associated basis functions must be zero. This is necessary to ensure conformity since these basis functions on the neighbouring, lower order, elements are not activated.

4.3. **H(curl)** *and* **H(div)**-*conforming subspaces*

The basis functions for an **H(curl)**-conforming subspace given in Table III are separated into subsets of basis functions associated with the edges, faces and element interior. As before, the connectivity mapping on element $\mathbf{t}$ may be partitioned into corresponding sub-blocks,

$$\mathbf{\Lambda}_{\mathbf{t}} = \mathtt{blockdiag}[\mathbf{\Lambda}_{\mathbf{t}}^{\mathbf{e}_1}, \ldots, \mathbf{\Lambda}_{\mathbf{t}}^{\mathbf{e}_6}, \mathbf{\Lambda}_{\mathbf{t}}^{\mathbf{f}_1}, \ldots, \mathbf{\Lambda}_{\mathbf{t}}^{\mathbf{f}_3}, \mathbf{\Lambda}_{\mathbf{t}}^{\mathbf{t}}] \tag{26}$$

The contributions from each entity are then constructed using the same procedure as for the space H^1, with the only difference being that the second row of Table IV is used to determine the number of degrees of freedom to be assigned.

In the same vein, the basis functions for an **H(div)**-conforming subspace given in Table VI are separated into subsets of basis functions associated with the faces and element interior and the connectivity mapping takes the form

$$\mathbf{\Lambda}_{\mathbf{t}} = \mathtt{blockdiag}[\mathbf{\Lambda}_{\mathbf{t}}^{\mathbf{f}_1}, \ldots, \mathbf{\Lambda}_{\mathbf{t}}^{\mathbf{f}_3}, \mathbf{\Lambda}_{\mathbf{t}}^{\mathbf{t}}] \tag{27}$$

The treatment is then identical with that for the H^1-case, using the third row of Table VI to determine the number of degrees of freedom.

It will be noticed that in passing from H^1 to **H(curl)** to **H(div)**, the entity with the lowest dimension is dropped at each step. One might wonder what happens in the next step whereby faces would be removed, yielding a mapping of the form

$$\mathbf{\Lambda}_{\mathbf{t}} = \mathtt{blockdiag}[\mathbf{\Lambda}_{\mathbf{t}}^{\mathbf{t}}] \tag{28}$$

This simply corresponds to the L_2 space considered earlier.

5. CONCLUSION

We have discussed the main problems in the construction of hierarchic bases for finite element discretization of the spaces H^1, **H(curl)**, **H(div)** and L_2 on tetrahedral elements. A simple

approach to ensuring conformity of the local finite element bases across element interfaces has been presented, based on a permutation of the local ordering of the global nodes. This approach circumvents many of the difficulties in constructing hierarchic bases, and means that we are able to construct hierarchic bases of arbitrary polynomial order. Furthermore, it is shown how appropriate local to global transformation are used to construct finite element approximations of arbitrary, non-uniform, local order approximation on unstructured meshes of curvilinear tetrahedral elements.

ACKNOWLEDGEMENTS

The support of this work by the Engineering and Physical Sciences Research Council of Great Britain under grant GR/M59426 is gratefully acknowledged.

REFERENCES

1. Bossavit A. *Computational Electromagnetism*: *Variational Formulation*, *Complementarity*, *Edge Elements*. Academic Press: New York, 1998.
2. Brezzi F, Fortin M. *Mixed and Hybrid Finite Element Methods*. Springer-Verlag: Berlin, 1991.
3. Jin J. *The Finite Element Method in Electromagnetics*. Wiley: New York, 1993.
4. Silvester P, Ferrari R. *Finite Elements for Electrical Engineers*. Cambridge University Press: Cambridge, 1996.
5. Schwab C. *p- and hp-finite element methods*: *theory and applications in solid and fluid mechanics*. Numerical Mathematics and Scientific Computation. Oxford University Press: Oxford, 1998.
6. Szabo B, Babuska I. *Finite Element Analysis*. Wiley: New York, 1991.
7. Karniadakis G, Sherwin S. *Spectral/hp Element Methods for CFD*. Oxford University Press: Oxford, 1999.
8. Nédélec J. Mixed finite elements in $\mathbb{R}^3$. *Numerische Mathematik* 1980; **93**:315–341.
9. Nédélec J. A new family of mixed finite elements in $\mathbb{R}^3$. *Numerische Mathematik* 1986; **50**:57–81.
10. Hiptmair R. Canonical construction of finite elements. *Mathematics of Computing* 1999; **68**(228):1325–1346.
11. Bossavit A. A rationale for edge-elements in 3-d fields computations. *IEEE Transactions on Magnetics* 1988; **24**(1):74–79.
12. Mur G. Edge elements, their advantages and their disadvantages. *IEEE Transactions on Magnetics* 1994; **30**(5):3552–3557.
13. Webb JP. Edge elements and what they can do for you. *IEEE Transactions on Antennas and Propagation* 1993; **29**:1460–1465.
14. Whitney H. *Geometric Integration Theory*. Princeton University Press: Princeton, 1957.
15. Cendes Z. Vector finite elements for electromagnetic field computation. *IEEE Transactions on Magnetics* 1991; **27**(5):3958–3967.
16. Geuzaine C, Meys B, Dular P, Legros W. Convergence of high order curl-conforming finite elements. *IEEE Transactions on Magnetics* 1999; **35**(3):1442–1444.
17. Kameari A. Calculation of transient 3D eddy current using edge-elements. *IEEE Transactions on Magnetics* 1990; **26**:466–469.
18. Lee J-F, Sun D-K, Cendes Z. Full-wave analysis of dielectric waveguides using tangential vector finite elements. *IEEE Transactions on Microwave Theory and Techniques* 1991; **39**(8):1262–1271.
19. Bossavit A, Mayergoyz I. Edge elements in scattering problems. *IEEE Transactions on Magnetics* 1989; **25**(4):2816–2821.
20. Kameari A. Symmetric second order edge elements for triangles and tetrahedra. *IEEE Transactions on Magnetics* 1999; **35**(3):1394–1397.
21. Lee J-F, Sun D-K, Cendes Z. Tangential vector finite elements for electromagnetic field computation. *IEEE Transactions on Magnetics* 1991; **27**(5):4032–4035.
22. Mur G, de Hoop A. A finite element method for three-dimensional electromagnetic fields in inhomogeneous media. *IEEE Transactions on Magnetics* 1985; **21**(6):2188–2191.
23. Webb JP, Forghani B. Hierarchical scalar and vector tetrahedra. *IEEE Transactions on Magnetics* 1993; **29**(2):1495–1498.
24. Andersen L, Volakis J. Hierarchical tangential vector finite elements for tetrahedra. *IEEE Microwave and Guided Wave Letters* 1998; **8**(3):127–129.
25. Graglia RD, Wilton DR, Peterson AF. Higher order interpolatory vector bases for computational electromagnetics. *IEEE Transactions on Antennas and Propagation* 1997; **45**(3):329–342.

26. Webb JP. Hierarchical vector basis functions of arbitrary order for triangular and tetrahedral finite elements. *IEEE Transactions on Antennas and Propagation* 1999; **47**(8):1244–1253.
27. Demkowicz L, Vardapetyan L. Modeling of electromagnetic absorption/scattering problems using hp-adaptive finite elements. *Computer Methods in Applied Mechanics and Engineering* 1998; **152**(1–2):103–124.
28. Demkowicz L, Monk P, Vardapetyan L, Rachowicz W. *De Rham diagram for hp finite element spaces*. Technical Report, TICAM Report 99-6, University of Texas at Austin, 1999.
29. Ainsworth M, Coyle J. Hierarchic hp-edge element families for Maxwell's equations on hybrid quadrilateral/triangular meshes. *Computer Methods in Applied Mechanics and Engineering* 2001; **190**:6709–6733.
30. Ciarlet PG. *The Finite Element Method for Elliptic Problems*. Elsevier, North-Holland: Amsterdam, 1978.
31. Akin JE. *Finite Elements in Analysis and Design*. Academic Press: New York, 1994.
32. Ainsworth M, Senior B. hp-Finite element procedures on non-uniform geometric meshes: adaptivity and constrained approximation. In *Grid Generation and Adaptive Algorithms*, Bern MW, Flaherty JE, Luskin M (eds), vol. 113. IMA: Minnesota, 1999; 1–29.
33. Gradshteyn IS, Ryzhik IM. In *Table of Integrals*, *Series and Products* (5th edn), Jeffrey A (ed.). Academic Press Ltd.: UK, 1994.
34. Marsden JE, Hughes TJR. *Mathematical Foundations of Elasticity*. Prentice-Hall: Englewood Cliffs, NJ, 1983.
35. Ainsworth M, Senior B. Aspects of an adaptive *hp*-finite element method: adaptive strategy, conforming approximation and efficient solvers. *Computer Methods in Applied Mechanics and Engineering* 1997; **150**:65–87.
36. Kron G. A set of principles to interconnect the solutions of physical systems. *Journal of Applied Physics* 1953; **24**(8):965–980.

